

Design of Multiple Unimodular Waveforms With Low Auto- and Cross-Correlations for Radar via Majorization-Minimization

Yongzhe Li^{†‡}, Sergiy A. Vorobyov[†], and Zishu He[‡]

[†]Dept. Signal Processing and Acoustics, Aalto University, P.O. Box 13000, FI-00076 Aalto, Finland

[‡]Dept. EE, University of Electronic Science and Technology of China, Chengdu, 611731, China

lyzlyz888@gmail.com/yongzhe.li@aalto.fi, svor@ieee.org, zshe@uestc.edu.cn

Abstract—We develop a new efficient method for designing unimodular waveforms with good auto- and cross-correlation properties for multiple-input multiple-output (MIMO) radar. Our waveform design scheme is conducted based on minimization of the integrated sidelobe level of designed waveforms, which is formulated as a quartic non-convex optimization problem. We start from simplifying the quartic optimization problem and then transform it into a quadratic form. By means of the majorization-minimization technique that seeks to find the solution of a corresponding quadratic optimization problem, we resolve the design of waveforms for MIMO radar. Corresponding algorithms that enable good correlations of the designed waveforms and meanwhile show faster convergence as compared to their counterparts are proposed and then tested.

I. INTRODUCTION

Waveform design has become a research field of significant interest in multiple-input multiple-output (MIMO) radar since the emergence of MIMO radar concept [1]–[5]. The application of waveform design plays an important role in MIMO radar (also in single-input single-output radar) signal processing because high-quality waveform can guarantee good localization accuracy [6], high resolution [7], and improved delay-Doppler ambiguity of the potential target [8]. Moreover, in harsh environment such as in the presence of heterogeneous clutter and active jamming, robust or adaptive waveform designs are capable of suppressing them [9]. One of the most important factors that determine the quality of designed waveforms is the correlation property, i.e., the auto- and cross-correlations between different time lags of the waveforms. Perfect or low waveform correlations mean that the waveforms launched from radar platform are uncorrelated to any non-zero time-delayed version of themselves, which ensures that the target at the range bin of interest can be easily extracted after matched filtering, and the sidelobes from other range bins have almost no effect on its attenuation. Despite the application of correlated waveforms in MIMO radar [8], [10], [11], uncorrelated waveforms are still the most preferable and they can be easily converted to correlated ones by weighting on them. On the other hand, unimodular waveforms are still preferable compared to other counterparts due to their constant energy at any time lag, which significantly reduces the cost of hardware.

There has been an extensive literature on waveform design for radar applications [12]–[19]. The integrated sidelobe

level (ISL), which characterizes the correlation properties of waveforms and evaluates the accumulated sidelobes at all non-zero time lags, is the most commonly used metric. To design waveforms via ISL minimization, the work of [13] has proposed to produce unimodular waveforms in frequency domain using a cyclic procedure of iterative calculations. The methods associated with ISL and weighted ISL minimization therein were named CAN and WeCAN, respectively. These methods were later extended to MIMO radar case based on the same idea of using cyclic procedure of iterative calculations [5]. The work of [18] dealt with the same ISL minimization problem as CAN for designing a single waveform but solved it via majorization-minimization (MaMi) technique [20]. This technique has previously been used in [17] where the design of multiple waveforms were implemented from information-theoretic perspective. The recent work of [19] has extended [18] to the case of multiple waveforms.

In this paper, we develop an efficient method for designing a set of unimodular waveforms with good auto- and cross-correlation properties, which can be applied to MIMO radar. We conduct the waveform design based on ISL minimization of the waveforms. Using proper modeling and some transformations, we formulate the ISL minimization based design as a quartic non-convex optimization problem. We show how to simplify the quartic optimization problem and then transform it into a quadratic form. By means of the MaMi technique which majorizes the objective function of the quadratic optimization problem and seeks to find the corresponding solution via iterative calculations, we resolve the formulated waveform design for MIMO radar. Corresponding algorithms that enable good correlations of the designed waveforms and meanwhile show faster convergence as compared to the existing counterparts are proposed and tested in terms of simulations.

II. SIGNAL MODEL AND PROBLEM FORMULATION

Consider a MIMO radar equipped with M transmit antenna elements from which a set of M unimodular waveforms, denoted by the $P \times M$ matrix $\mathbf{Y} \triangleq [\mathbf{y}_1, \dots, \mathbf{y}_M]$, is launched within a pulse duration. Here \mathbf{y}_m , $m \in \{1, \dots, M\}$ stands for the $P \times 1$ emitted waveform vector associated with the m th antenna and P is the code length of each waveform. Let the p th ($p \in \{1, \dots, P\}$) element of \mathbf{y}_m that is associated with the

p th sub-pulse be $y_m(p) = e^{j\psi_m(p)}$ where $\psi_m(p)$ is an arbitrary phase value ranging between $-\pi$ and π . The main issue of the waveform design for MIMO radar lies in synthesizing sequences $\{y_m(p)\}_{m=1, p=1}^{M, P}$ which have good auto- and cross-correlation properties.

The ISL of the waveforms $\{y_m(p)\}_{m=1, p=1}^{M, P}$ is expressed as

$$\zeta = \sum_{m=1}^M \sum_{\substack{p=-P+1 \\ p \neq 0}}^{P-1} |r_{mm}(p)|^2 + \sum_{m=1}^M \sum_{\substack{m'=1 \\ m' \neq m}}^M \sum_{p=-P+1}^{P-1} |r_{mm'}(p)|^2 \quad (1)$$

where $r_{mm'}(p) \triangleq \sum_{k=p+1}^P y_m(k) y_{m'}^*(k-p)$, $m, m' \in \{1, \dots, M\}$; $p \in \{1, \dots, P-1\}$ stands for the cross-correlation level of the m th and m' th waveforms at the p th time lag, and $|\cdot|$ and $(\cdot)^*$ are modulus and conjugation operators, respectively. Note that the first component of the sum on the right hand side of (1) stands for the ISL associated with auto-correlations and the latter represents the ISL associated with cross-correlations.

Using matrix expressions, the ISL ζ in (1) can be rewritten into the following compact form

$$\zeta = \sum_{p=-P+1}^{P-1} \|\mathbf{R}_p - P\mathbf{I}_M \delta_p\|^2 \quad (2)$$

where the $M \times M$ waveform correlation matrix \mathbf{R}_p , $p \in \{-P+1, \dots, 0, \dots, P-1\}$ is constructed as

$$\mathbf{R}_p \triangleq \begin{bmatrix} r_{11}(p) & r_{12}(p) & \dots & r_{1M}(p) \\ r_{21}(p) & r_{22}(p) & \dots & r_{2M}(p) \\ \vdots & \vdots & \ddots & \vdots \\ r_{M1}(p) & \dots & \dots & r_{MM}(p) \end{bmatrix} \quad (3)$$

δ_p is the Kronecker delta function whose value is 1 only when $p = 0$ while otherwise it is 0, \mathbf{I}_M is the $M \times M$ identity matrix, and $\|\cdot\|$ stands for the Frobenius norm of a matrix.

Transforming (2) into frequency domain and performing some derivations, the ISL can be expressed as [5]

$$\zeta = \frac{1}{2P} \sum_{p=1}^{2P} \|\tilde{\mathbf{y}}(\omega_p) \tilde{\mathbf{y}}^H(\omega_p) - P\mathbf{I}_M\|^2 \quad (4)$$

where $\omega_p \triangleq \frac{2\pi}{2P}p$ and $\tilde{\mathbf{y}}(\omega_p) \triangleq \sum_{n=1}^P \tilde{\mathbf{y}}_n e^{-j\omega_p n}$ with $\tilde{\mathbf{y}}_n$ constructed by the n th row of the waveform matrix \mathbf{Y} which is explicitly expressed as $\tilde{\mathbf{y}}_n \triangleq [y_1(n), \dots, y_M(n)]^T$. Here $(\cdot)^T$ and $(\cdot)^H$ are transpose and conjugate transpose operators, respectively.

Expanding the squared norm in (4), the ISL can be expressed in the following form

$$\zeta = \frac{1}{2P} \sum_{p=1}^{2P} \left(\|\tilde{\mathbf{y}}(\omega_p)\|^4 - 2P \|\tilde{\mathbf{y}}(\omega_p)\|^2 + P^2 M \right) \quad (5)$$

which can be further rewritten as the following compact form

$$\zeta = \frac{1}{2P} \sum_{p=1}^{2P} \left((\mathbf{y}^H \mathbf{A}_p \mathbf{A}_p^H \mathbf{y})^2 - 2P (\mathbf{y}^H \mathbf{A}_p \mathbf{A}_p^H \mathbf{y}) + P^2 M \right) \quad (6)$$

where $\mathbf{y} \triangleq \text{vec}(\mathbf{Y}) = [\mathbf{y}_1^T, \dots, \mathbf{y}_M^T]^T$ is the $MP \times 1$ vectorized version of the waveform matrix \mathbf{Y} , $\mathbf{A}_p \triangleq \mathbf{I}_M \otimes \mathbf{a}_p$ is an $MP \times M$ matrix with $\mathbf{a}_p \triangleq [1, e^{j\omega_p}, \dots, e^{j(P-1)\omega_p}]^T$, and $\text{vec}(\cdot)$ and \otimes are respectively vectorization and Kronecker product operators. Note that the results $\tilde{\mathbf{y}}(\omega_p) = \mathbf{A}_p^H \mathbf{y}$ and $\|\tilde{\mathbf{y}}(\omega_p)\|^2 = \tilde{\mathbf{y}}^H(\omega_p) \tilde{\mathbf{y}}(\omega_p)$ have been used to obtain (6) from (5).

We can finally express the waveform design problem associated with ISL minimization as

$$\min_{\mathbf{y}} \zeta \quad \text{s.t.} \quad |\mathbf{y}(p')| = 1, \quad p' = 1, \dots, MP. \quad (7)$$

III. WAVEFORM DESIGN VIA MAMI

In order to solve (7) efficiently, we start by simplifying (6). To begin, we note that the following train of equalities

$$\begin{aligned} \sum_{p=1}^{2P} (\mathbf{y}^H \mathbf{A}_p \mathbf{A}_p^H \mathbf{y}) &= \mathbf{y}^H \sum_{p=1}^{2P} (\mathbf{A}_p \mathbf{A}_p^H) \mathbf{y} \\ &= \|\mathbf{y}\|^2 = 2MP^2 \end{aligned} \quad (8)$$

holds because of the property $\sum_{p=1}^{2P} (\mathbf{A}_p \mathbf{A}_p^H) = 2P\mathbf{I}_{MP}$. Therefore, the latter two components of the sum in (6) are immaterial for optimization. After ignoring them in (6), the corresponding optimization problem can be rewritten as

$$\begin{aligned} \min_{\mathbf{y}} \quad & \sum_{p=1}^{2P} (\mathbf{y}^H \mathbf{A}_p \mathbf{A}_p^H \mathbf{y})^2 \\ \text{s.t.} \quad & |\mathbf{y}(p')| = 1, \quad p' = 1, \dots, MP. \end{aligned} \quad (9)$$

The objective function in (9) takes a quartic form with respect to \mathbf{y} , and it can be transformed to the following form

$$\begin{aligned} \sum_{p=1}^{2P} (\mathbf{y}^H \mathbf{A}_p \mathbf{A}_p^H \mathbf{y})^2 &= \sum_{p=1}^{2P} \text{tr}^2 \{ \tilde{\mathbf{Y}}^H \mathbf{A}_p \mathbf{A}_p^H \} \\ &= \sum_{p=1}^{2P} \text{vec}^H(\tilde{\mathbf{Y}}) \text{vec}(\mathbf{A}_p \mathbf{A}_p^H) \text{vec}^H(\mathbf{A}_p \mathbf{A}_p^H) \text{vec}(\tilde{\mathbf{Y}}) \\ &\triangleq \text{vec}^H(\tilde{\mathbf{Y}}) \Phi \text{vec}(\tilde{\mathbf{Y}}) \end{aligned} \quad (10)$$

where $\tilde{\mathbf{Y}} \triangleq \mathbf{y}\mathbf{y}^H$ is an $MP \times MP$ rank-1 matrix, $\Phi \triangleq \sum_{p=1}^{2P} \text{vec}(\mathbf{A}_p \mathbf{A}_p^H) \text{vec}^H(\mathbf{A}_p \mathbf{A}_p^H)$ is an $M^2 P^2 \times M^2 P^2$ matrix, and $\text{tr}\{\cdot\}$ stands for the matrix trace. The properties $\mathbf{y}^H \mathbf{A}_p \mathbf{A}_p^H \mathbf{y} = \text{tr}\{\tilde{\mathbf{Y}}^H \mathbf{A}_p \mathbf{A}_p^H\} = \text{vec}^H(\tilde{\mathbf{Y}}) \text{vec}(\mathbf{A}_p \mathbf{A}_p^H)$ have been used in the derivations of (10). Therefore, the optimization problem (9) can be further rewritten as

$$\min_{\tilde{\mathbf{Y}}} \text{vec}^H(\tilde{\mathbf{Y}}) \Phi \text{vec}(\tilde{\mathbf{Y}}) \quad (11a)$$

$$\text{s.t.} \quad \tilde{\mathbf{Y}} = \mathbf{y}\mathbf{y}^H \quad (11b)$$

$$|\mathbf{y}(p')| = 1, \quad p' = 1, \dots, MP. \quad (11c)$$

Before applying majorization to the objective function (11a), we present the following result to be used later [18].

The quadratic function $\mathbf{x}^H \mathbf{Q} \mathbf{x}$ is majorized by the function $\mathbf{x}^H \mathbf{G} \mathbf{x} + 2\Re(\mathbf{x}^H (\mathbf{Q} - \mathbf{G}) \mathbf{x}_0) + \mathbf{x}_0^H (\mathbf{G} - \mathbf{Q}) \mathbf{x}_0$ at \mathbf{x}_0 when the generalized inequality $\mathbf{G} \succeq \mathbf{Q}$ is satisfied. Here \mathbf{G} and \mathbf{Q} are Hermitian positive semidefinite matrices.

It can be shown that the largest eigenvalue of Φ , denoted by $\lambda_{\max}(\Phi)$, equals $2MP^2$. We omit the proof because of the space limitation. Therefore, we can select $\mathbf{G} \triangleq \lambda_{\max}(\Phi)\mathbf{I}_{M^2P^2}$ to guarantee the generalized inequality $\mathbf{G} \succeq \Phi$. Using the above-mentioned majorization result, the objective function (11a) can be majorized as

$$g_1(\tilde{\mathbf{Y}}, \tilde{\mathbf{Y}}^{(k)}) = \lambda_{\max}(\Phi) \text{vec}^H(\tilde{\mathbf{Y}}) \text{vec}(\tilde{\mathbf{Y}}) + 2\Re\{\text{vec}^H(\tilde{\mathbf{Y}})(\Phi - \lambda_{\max}(\Phi)\mathbf{I}_{M^2P^2})\text{vec}(\tilde{\mathbf{Y}}^{(k)})\} + \text{vec}^H(\tilde{\mathbf{Y}}^{(k)})(\lambda_{\max}(\Phi)\mathbf{I}_{M^2P^2} - \Phi)\text{vec}(\tilde{\mathbf{Y}}^{(k)}) \quad (12)$$

where the matrix $\tilde{\mathbf{Y}}^{(k)} \triangleq \mathbf{y}^{(k)}(\mathbf{y}^{(k)})^H$ is obtained at the k th iteration and $\Re\{\cdot\}$ denotes the real part of a complex value. Note that $\text{vec}^H(\tilde{\mathbf{Y}})\text{vec}(\tilde{\mathbf{Y}}) = \|\mathbf{y}\|^4 = M^2P^2$. Hence, both the first and third components of the sum in (12) are constant terms which are immaterial for optimization. The problem (11) can be therefore rewritten as

$$\min_{\tilde{\mathbf{Y}}} \text{vec}^H(\tilde{\mathbf{Y}})(\Phi - \lambda_{\max}(\Phi)\mathbf{I}_{M^2P^2})\text{vec}(\tilde{\mathbf{Y}}^{(k)}) \quad (13a)$$

$$\text{s.t. } \tilde{\mathbf{Y}} = \mathbf{y}\mathbf{y}^H \quad (13b)$$

$$|\mathbf{y}(p')| = 1, \quad p' = 1, \dots, MP. \quad (13c)$$

Using the properties $\text{vec}(\tilde{\mathbf{Y}}) = \text{vec}(\mathbf{y}\mathbf{y}^H) = (\mathbf{y}^T \otimes \mathbf{I}_{MP})^H \mathbf{y}$ and $\text{vec}(\mathbf{A}_p \mathbf{A}_p^H) = (\mathbf{A}_p^T \otimes \mathbf{I}_{MP})^H \text{vec}(\mathbf{A}_p)$, and also substituting the explicit expressions of Φ and $\lambda_{\max}(\Phi)$, the objective function (13a) can be further transformed as

$$\begin{aligned} & \text{vec}^H(\tilde{\mathbf{Y}})(\Phi - \lambda_{\max}(\Phi)\mathbf{I}_{M^2P^2})\text{vec}(\tilde{\mathbf{Y}}^{(k)}) \\ &= \sum_{p=1}^{2P} \left(\mathbf{y}^H(\mathbf{y}^T \otimes \mathbf{I}_{MP})(\mathbf{A}_p^T \otimes \mathbf{I}_{MP})^H \text{vec}(\mathbf{A}_p) \text{vec}^H(\mathbf{A}_p) \right. \\ & \quad \times (\mathbf{A}_p^T \otimes \mathbf{I}_{MP})((\mathbf{y}^{(k)})^T \otimes \mathbf{I}_{MP})^H \mathbf{y}^{(k)} \\ & \quad \left. - 2MP^2 \mathbf{y}^H(\mathbf{y}^T \otimes \mathbf{I}_{MP})((\mathbf{y}^{(k)})^T \otimes \mathbf{I}_{MP})^H \mathbf{y}^{(k)} \right) \\ &= \sum_{p=1}^{2P} \mathbf{y}^H((\mathbf{y}^T \mathbf{A}_p^*) \otimes \mathbf{I}_{MP}) \text{vec}(\mathbf{A}_p) \text{vec}^H(\mathbf{A}_p)((\mathbf{A}_p^T(\mathbf{y}^{(k)})^*) \\ & \quad \otimes \mathbf{I}_{MP})\mathbf{y}^{(k)} - 2MP^2 \mathbf{y}^H(\mathbf{y}^T(\mathbf{y}^{(k)})^*)\mathbf{y}^{(k)} \quad (14) \end{aligned}$$

$$= \sum_{p=1}^{2P} \mathbf{y}^H \mathbf{A}_p ((\mathbf{y}^{(k)})^H \mathbf{A}_p \mathbf{A}_p^H \mathbf{y}^{(k)}) \mathbf{A}_p^H \mathbf{y} - 2MP^2 \mathbf{y}^H (\mathbf{y}^{(k)} (\mathbf{y}^{(k)})^H) \mathbf{y} \quad (15)$$

where the mixed product property of Kronecker product and the property $((\mathbf{y}^T \mathbf{A}_p^*) \otimes \mathbf{I}_{MP}) \text{vec}(\mathbf{A}_p) = \mathbf{A}_p \mathbf{A}_p^H \mathbf{y}$ are used to derive (14) and (15), respectively.

Stacking \mathbf{A}_p , $p = 1, \dots, 2P$ into a new $MP \times 2MP$ matrix \mathbf{A} , i.e., $\mathbf{A} \triangleq [\mathbf{A}_1, \dots, \mathbf{A}_{2P}]$, (15) can be further rewritten in the following compact form

$$\begin{aligned} & \sum_{p=1}^{2P} \mathbf{y}^H \mathbf{A}_p ((\mathbf{y}^{(k)})^H \mathbf{A}_p \mathbf{A}_p^H \mathbf{y}^{(k)}) \mathbf{A}_p^H \mathbf{y} \\ & \quad - 2MP^2 \mathbf{y}^H (\mathbf{y}^{(k)} (\mathbf{y}^{(k)})^H) \mathbf{y} \\ &= \mathbf{y}^H (\mathbf{A} \mathbf{A}^{(k)} \mathbf{A}^H - 2MP^2 \mathbf{y}^{(k)} (\mathbf{y}^{(k)})^H) \mathbf{y} \quad (16) \end{aligned}$$

where the $2MP \times 2MP$ diagonal matrix $\mathbf{A}^{(k)}$ is expressed as

$$\mathbf{A}^{(k)} \triangleq \text{diag}\left\{ \|\mathbf{a}_1^H \tilde{\mathbf{Y}}^{(k)}\|^2 \mathbf{1}_M^T, \dots, \|\mathbf{a}_{2P}^H \tilde{\mathbf{Y}}^{(k)}\|^2 \mathbf{1}_M^T \right\} \quad (17)$$

with $\mathbf{1}_M$ denoting a vector whose M elements are all ones. Therefore, the optimization problem (13) can be rewritten as

$$\min_{\mathbf{y}} \mathbf{y}^H (\mathbf{A} \mathbf{A}^{(k)} \mathbf{A}^H - 2MP^2 \mathbf{y}^{(k)} (\mathbf{y}^{(k)})^H) \mathbf{y} \quad (18a)$$

$$\text{s.t. } |\mathbf{y}(p')| = 1, \quad p' = 1, \dots, MP. \quad (18b)$$

Applying the previous majorization result to the first component of the quadratic objective function (18a) and selecting $\mathbf{G} \triangleq \mu_{\max}^{(k)} \mathbf{A} \mathbf{A}^H$ with $\mu_{\max}^{(k)} \triangleq \max\{\|\mathbf{a}_1^H \tilde{\mathbf{Y}}^{(k)}\|^2 \mathbf{1}_M^T, \dots, \|\mathbf{a}_{2P}^H \tilde{\mathbf{Y}}^{(k)}\|^2 \mathbf{1}_M^T\}$, we guarantee that $\mathbf{G} \succeq \mathbf{A} \mathbf{A}^{(k)} \mathbf{A}^H$. Therefore, the objective function (18a) is majorized as

$$\begin{aligned} g_2(\mathbf{y}, \mathbf{y}^{(k)}) &= \mu_{\max}^{(k)} \mathbf{y}^H \mathbf{A} \mathbf{A}^H \mathbf{y} + 2\Re\{\mathbf{y}^H (\mathbf{A}(\mathbf{A}^{(k)} - \mu_{\max}^{(k)} \mathbf{I}_{2MP}) \mathbf{A}^H \\ & \quad - 2MP^2 \mathbf{y}^{(k)} (\mathbf{y}^{(k)})^H) \mathbf{y}^{(k)}\} + (\mathbf{y}^{(k)})^H (2MP^2 \mathbf{y}^{(k)} \\ & \quad \times (\mathbf{y}^{(k)})^H - \mathbf{A}(\mathbf{A}^{(k)} - \mu_{\max}^{(k)} \mathbf{I}_{2MP}) \mathbf{A}^H) \mathbf{y}^{(k)}. \quad (19) \end{aligned}$$

Note that $\mathbf{A} \mathbf{A}^H = \sum_{p=1}^{2P} \mathbf{A}_p \mathbf{A}_p^H = 2P \mathbf{I}_{MP}$ and $\mathbf{y}^H \mathbf{y} = (\mathbf{y}^{(k)})^H \mathbf{y}^{(k)} = \|\mathbf{y}\|^2 = MP$. Hence the first and third components of the sum in (19) are immaterial for optimization. The optimization problem (18) can be finally simplified as

$$\begin{aligned} \min_{\mathbf{y}} \mathbf{y}^H \mathbf{z}^{(k)} \\ \text{s.t. } |\mathbf{y}(p')| = 1, \quad p' = 1, \dots, MP. \quad (20) \end{aligned}$$

where $\mathbf{z}^{(k)} \triangleq -\mathbf{A} \mathbf{A}^{(k)} \mathbf{A}^H \mathbf{y}^{(k)} + 2\mu_{\max}^{(k)} P \mathbf{y}^{(k)} + 2M^2 P^3 \mathbf{y}^{(k)}$. Due to the constant modulus property of \mathbf{y} , (20) is equivalent to the following optimization problem

$$\begin{aligned} \min_{\mathbf{Y}} \|\mathbf{Y} - \mathbf{Z}^{(k)}\|^2 \\ \text{s.t. } |[\mathbf{Y}]_{m,p}| = 1, \quad m = 1, \dots, M; p = 1, \dots, P \quad (21) \end{aligned}$$

where

$$\mathbf{Z}^{(k)} \triangleq -\mathbf{A} \mathbf{A}^{(k)} \mathbf{A}^H \mathbf{Y}^{(k)} + 2\mu_{\max}^{(k)} P \mathbf{Y}^{(k)} + 2M^2 P^3 \mathbf{Y}^{(k)} \quad (22)$$

with the waveform matrix $\mathbf{Y}^{(k)}$ achieved at the k th iteration and $[\cdot]_{m,p}$ standing for the (m, p) th element of a matrix. The solution of (21) can be found in the following closed form

$$[\mathbf{Y}]_{m,p} = e^{j \arg([\mathbf{Z}^{(k)}]_{m,p})}, \quad m = 1, \dots, M; p = 1, \dots, P. \quad (23)$$

Note that (21) and (22) are written into matrix forms which facilitate our proposed algorithm in the following. Based on the above derivations, we propose an original algorithm for the ISL minimization problem (7) via MaMi technique summarized in Algorithm 1. To speed up the convergence of this algorithm, we can resort to accelerated schemes. For example, the schemes in [18] which lead to efficient accelerated methods can be used. Here we summarize also our algorithm accelerated by fix-point scheme in Algorithms 2. We refer interested readers to [18] for the proof of convergence.

Algorithm 1 ISL minimization via MaMi

```

1:  $k \leftarrow 0$ ,  $\mathbf{Y} \leftarrow P \times M$  unimodular sequence matrix with
   random phases.
2: repeat
3:   procedure ISLMaMi( $\mathbf{Y}^{(k)}$ )
4:      $\mu_{\max}^{(k)} = \max\{\|\mathbf{a}_p^H \tilde{\mathbf{Y}}^{(k)}\|^2\}_{p=1}^{2P}$ 
5:      $\mathbf{Z}^{(k)} = -\mathbf{A}\mathbf{\Lambda}^{(k)}\mathbf{A}^H\mathbf{Y}^{(k)} + 2\mu_{\max}^{(k)}P\mathbf{Y}^{(k)}$ 
6:        $+ 2M^2P^3\mathbf{Y}^{(k)}$ 
7:      $[\mathbf{Y}^{(k+1)}]_{m,p} = e^{j\arg([\mathbf{Z}^{(k)}]_{m,p})}$ ,  $m = 1, \dots, M$ ;
8:        $p = 1, \dots, P$ .
9:      $k \leftarrow k + 1$ 
10:   end procedure
11: until convergence

```

IV. SIMULATION RESULTS

In our simulations, we compare the performance of our proposed waveform design algorithm with that of CAN (see [5]) and the method in [19] (named as CANSong), and also present correlation properties of the waveforms generated by them. We generate unimodular sequences with random phases as the initialization for each tested design, and the same initialized sequence is used when conducting comparison. The basic method of our work, i.e., Algorithm 1, and that of [19] (see Algorithm 3 therein) converge more slowly than the corresponding accelerated algorithms while giving similar minimized ISL performance. Therefore, we use the fix-point accelerated scheme. Two stopping criteria are employed in the conducted comparisons. One is the absolute ISL difference between the current and previous iterations normalized to the initial ISL, whose threshold is set to be 10^{-8} . The other is the norm of the difference between the waveform matrices obtained at the current and previous iterations, whose threshold is set to be 10^{-3} . All simulations for the tested methods are conducted based on the same hardware and software platforms, and are averaged by running 50 independent trials.

In the first example, we evaluate the convergence properties (i.e., running time versus code length) of the three tested waveform designs using the first (ISL based) stopping criterion. The number of designed waveforms is $M = 4$, and the code length P is varying from 20 to 200 with step size 20. Fig. 1 shows the performance comparison of the three waveform design. It can be seen from Fig. 1(a) that our proposed design and the design of [19] always outperform the CAN design in convergence rate in terms of the consumed time. It costs our proposed waveform design nearly the same running time as the design of [19] to obtain optimized waveforms when the code length is relatively smaller (i.e., from 20 to 80). However, our proposed design behaves increasingly better than the method of [19] when larger code length is selected, and indeed this superiority becomes obvious when both the code length and the number of waveforms are significantly large. Fig. 1(b) shows the corresponding achieved ISL of the three tested waveform

Algorithm 2 ISL minimization via accelerated MaMi

```

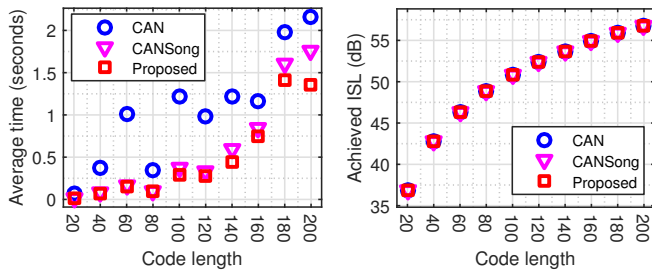
1:  $k \leftarrow 0$ ,  $\mathbf{Y} \leftarrow P \times M$  unimodular sequence matrix with
   random phases.
2: repeat
3:   procedure ISLAFMaMi( $\mathbf{Y}^{(k)}$ )
4:      $\hat{\mathbf{Y}} = \text{ISLMaMi}(\mathbf{Y}^{(k)})$ 
5:      $\hat{\hat{\mathbf{Y}}} = \text{ISLMaMi}(\hat{\mathbf{Y}})$ 
6:      $\hat{\Delta} = \hat{\mathbf{y}} - \mathbf{y}^{(k)}$ ;  $\hat{\hat{\Delta}} = \hat{\hat{\mathbf{Y}}} + \mathbf{Y}^{(k)} - 2\hat{\mathbf{Y}}$ 
7:      $\beta = -\|\hat{\Delta}\|/\|\hat{\hat{\Delta}}\|$ 
8:      $\mathbf{Z}^{(k)} = \mathbf{Y}^{(k)} - 2\beta\hat{\Delta} + \beta^2\hat{\hat{\Delta}}$ 
9:      $[\bar{\mathbf{Y}}^{(k)}]_{m,p} = e^{j\arg([\mathbf{Z}^{(k)}]_{m,p})}$ ,  $m = 1, \dots, M$ ;
10:        $p = 1, \dots, P$ .
11:   while  $\text{ISL}(\bar{\mathbf{Y}}^{(k)}) > \text{ISL}(\mathbf{Y}^{(k)})$  do
12:      $\beta \leftarrow (\beta - 1)/2$ 
13:      $\mathbf{Z}^{(k)} = \mathbf{Y}^{(k)} - 2\beta\hat{\Delta} + \beta^2\hat{\hat{\Delta}}$ 
14:      $[\bar{\mathbf{Y}}^{(k)}]_{m,p} = e^{j\arg([\mathbf{Z}^{(k)}]_{m,p})}$ ,  $m = 1, \dots, M$ ;
15:        $p = 1, \dots, P$ .
16:   end while
17:    $\mathbf{Y}^{(k+1)} = \bar{\mathbf{Y}}^{(k)}$ 
18:    $k \leftarrow k + 1$ 
19: end procedure
20: until convergence

```

designs. It can be seen from Fig. 1(b) that the three designs nearly achieve the same ISL, where the results are shown with overlapping graphic shapes. Indeed, the ISLs achieved by our proposed design and that of [19] are better than that achieved by the CAN algorithm, however, the difference is quite small (less than 10^{-4} dB).

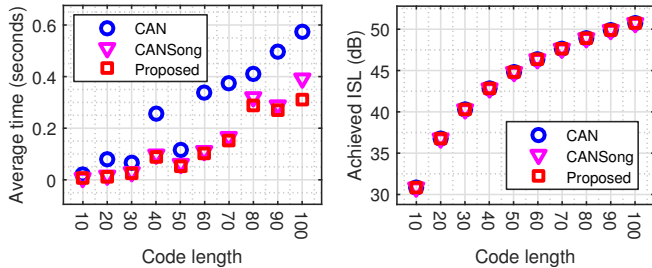
In the second example, we evaluate the convergence properties of the three tested designs using the second (waveform based) stopping criterion. The number of waveforms is $M = 2$, and the code length P is varying from 10 to 100 with step size 10. Fig. 2 shows the performance comparisons of the three waveform designs. Similar to Fig. 1, it can be seen from Fig. 2(a) that both our proposed design and the design of [19] outperform the CAN design in convergence rate with respect to the consumed time, and again our proposed design behaves increasingly better than that of [19] for larger code lengths. It can also be seen from Fig. 2(b) that the obtained ISL of the three tested designs are again quite close to each other, and the corresponding difference is smaller. Compared to the previous results, we remark that using the waveform based stopping criterion to obtain a desired ISL for all these waveform designs is generally faster than the case using the ISL based criterion.

In the third example, we present the correlation properties of waveforms optimized by the three tested designs using the ISL based stopping criterion. The corresponding waveform design parameters are $M = 2$ and $P = 256$. The normalized auto- and cross-correlations of the two designed waveforms are



(a) Running time versus code length. (b) Achieved ISL versus code length.

Fig. 1. Performance evaluation using the first stopping criterion.



(a) Running time versus code length. (b) Achieved ISL versus code length.

Fig. 2. Performance evaluation using the second stopping criterion.

shown in the sub figures of Fig. 3. It can be seen from Fig. 3 that the auto- and cross-correlations for the three tested designs are close to each other, which coincides with the ISL results in the previous two examples. The worst sidelobe level for the auto-correlation is about -23 dB, while the worst sidelobe level for the cross-correlations is around -20 dB.

V. CONCLUSION

An efficient method for designing multiple unimodular waveforms with good correlation properties that can be used for MIMO radar has been developed. We have employed ISL minimization of the waveforms as the designing criterion, and have formulated the ISL minimization based design as a quartic optimization problem. This quartic optimization problem has been converted into a quadratic form and then solved by means of MaMi technique. We have properly selected the majorized function for the objective function of the quadratic optimization problem, which is used by MaMi in order to find the corresponding solution. The proposed algorithms have shown good correlations of the designed waveforms and faster convergence as compared to its counterparts.

REFERENCES

- [1] P. Stoica, J. Li, and Y. Xie, "On probing signal design for MIMO radar," *IEEE Trans. Signal Process.*, vol. 55, no. 8, pp. 4151–4161, Aug. 2007.
- [2] Y. Yang and R. S. Blum, "MIMO radar waveform design based on mutual information and minimum mean-square error estimation," *IEEE Trans. Aerosp. Electron. Syst.*, vol. 43, no. 1, pp. 330–343, Jan. 2007.
- [3] B. Friedlander, "Waveform design for MIMO radars," *IEEE Trans. Aerosp. Electron. Syst.*, vol. 43, no. 3, pp. 1227–1238, Jul. 2007.
- [4] C.-Y. Chen and P. P. Vaidyanathan, "MIMO radar ambiguity properties and optimization using frequency-hopping waveforms," *IEEE Trans. Signal Process.*, vol. 56, no. 12, pp. 5926–5936, Dec. 2008.
- [5] H. He, P. Stoica, and J. Li, "Designing unimodular sequence sets with good correlations—Including an application to MIMO radar," *IEEE Trans. Signal Process.*, vol. 57, no. 11, pp. 4391–4405, Nov. 2009.
- [6] I. Bekkerman and J. Tabrikian, "Target detection and localization using MIMO radar and sonars," *IEEE Trans. Signal Process.*, vol. 54, no. 10, pp. 3873–3883, Oct. 2006.
- [7] J. Li, P. Stoica, and X. Zheng, "Signal synthesis and receiver design for MIMO radar imaging," *IEEE Trans. Signal Process.*, vol. 56, no. 8, pp. 3959–3968, Aug. 2008.
- [8] Y. Li, S. A. Vorobyov, and V. Koivunen, "Ambiguity function of the transmit beamspace-based MIMO radar," *IEEE Trans. Signal Process.*, vol. 63, no. 17, pp. 4445–4457, Sep. 2015.
- [9] D. DeLong and E. M. Hofstetter, "On the design of optimum radar waveforms for clutter rejection," *IEEE Trans. Inf. Theory*, vol. 13, no. 3, pp. 454–463, Jul. 1967.
- [10] A. Hassanien and S. A. Vorobyov, "Transmit energy focusing for DOA estimation in MIMO radar with colocated antennas," *IEEE Trans. Signal Process.*, vol. 59, no. 6, pp. 2669–2682, Jun. 2011.
- [11] S. Ahmed, J. S. Thompson, Y. R. Petillot, and B. Mulgrew, "Unconstrained synthesis of covariance matrix for MIMO radar transmit beampattern," *IEEE Trans. Signal Process.*, vol. 59, no. 8, pp. 3837–3849, Aug. 2011.
- [12] N. Levanon and E. Mozeson, *Radar Signals*. Hoboken, NJ, USA: Wiley, 2004.
- [13] P. Stoica, H. He, and J. Li, "New algorithms for designing unimodular sequences with good correlation properties," *IEEE Trans. Signal Process.*, vol. 57, no. 4, pp. 1415–1425, Apr. 2009.
- [14] A. De Maio, S. D. Nicola, Y. Huang, Z.-Q. Luo, and S. Zhang, "Design of phase codes for radar performance optimization with a similarity constraint," *IEEE Trans. Signal Process.*, vol. 57, no. 2, pp. 610–621, Feb. 2009.
- [15] A. Aubry, A. De Maio, A. Farina, and M. Wicks, "Knowledge-aided (potentially cognitive) transmit signal and receive filter design in signal-dependent clutter," *IEEE Trans. Aerosp. Electron. Syst.*, vol. 49, no. 1, pp. 93–117, Jan. 2013.
- [16] W. Rowe, P. Stoica, and J. Li, "Spectrally constrained waveform design," *IEEE Signal Process. Mag.*, vol. 31, no. 3, pp. 157–162, May 2014.
- [17] M. M. Naghsh, M. Modarres-Hashemi, S. ShahbazPanahi, M. Soltanalian, and P. Stoica, "Unified optimization framework for multi-static radar code design using information-theoretic criteria," *IEEE Trans. Signal Process.*, vol. 61, no. 21, pp. 5401–5416, Nov. 2013.
- [18] J. Song, P. Babu, and D. P. Palomar, "Optimization methods for designing sequences with low autocorrelation sidelobes," *IEEE Trans. Signal Process.*, vol. 63, no. 15, pp. 3998–4009, Aug. 2015.
- [19] J. Song, P. Babu, and D. P. Palomar, "Sequence set design with good correlation properties via majorization-minimization," *IEEE Trans. Signal Process.*, vol. 64, no. 11, pp. 2886–2879, Jun. 2016.
- [20] D. R. Hunter and K. Lange, "A tutorial on MM algorithms," *Amer. Statist.*, vol. 58, no. 1, pp. 30–37, Feb. 2004.

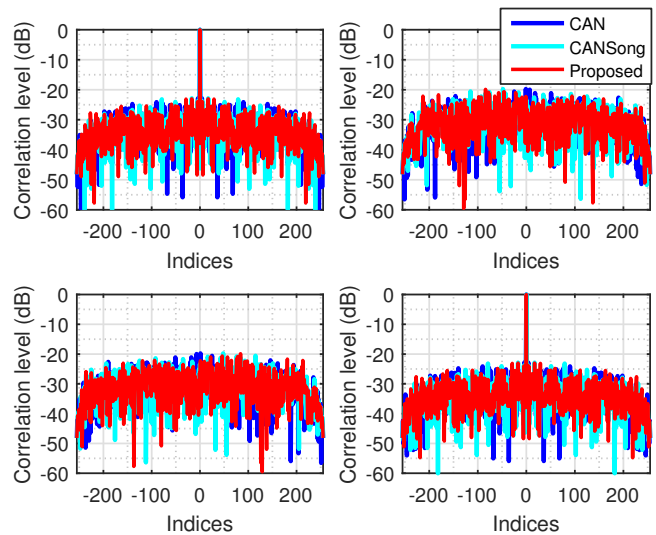


Fig. 3. Waveform correlations versus time lags.